

AIAA 80-0453R

Experiments in a Subscale Pilot Gust Tunnel

Hermann Viets,* Mont Ball,† and Michael Piatt‡
Wright State University, Dayton, Ohio

Introduction

THE development of a time dependent flow test facility has been attempted by a variety of methods. Mitchell¹ employed a technique in which the model was moved in relation to the flow, passing orthogonally through an open jet wind tunnel. Gilman and Bennett² employed a tunnel in which the gusts were produced by a set of airfoils mounted in a biplane arrangement on the opposite walls of a wind tunnel. As these airfoils were oscillated in a sinusoidal fashion, they induced an oscillating flow between them. Other methods include employing moving sinusoidal waves in the test section walls,³ oscillating the inlet section of an open circuit tunnel,⁴ an oscillating array of airfoils,⁵ and circulation control on a set of elliptical airfoils.⁶

The method which is probably the closest to that of the present investigation is due to Simmons and Platzer,⁷ who employed a pair of jet flaps. Each of the jet flaps is a fluidically oscillating jet driven by a pair of control jets, one on either side.

As a consequence of an effort to develop fluidically controlled time dependent jets for application to several diverse problems,^{8,9} a new technique was proposed for the construction of a high frequency gust tunnel.¹⁰ The method of operation of the fluidic nozzle is as follows: the flow passes through the throat of the jet nozzle (Fig. 1) and into a rapid expansion region. Because of the relative proximity of the walls, the flow must attach to one side of the expanded region or the other. This bistable condition can be strongly influenced by a small pressure difference between the two sides of the expanded channel. In a normal fluidic oscillator or a fluidically oscillating jet,^{8,11} this pressure difference is supplied by a feedback system between the two sides. In the present case, this pressure difference is created by the rotating valves shown on each side of the jet. The valves are rotated out of phase with each other, so that one is open when the other is closed. The resulting flow always attaches to the closed side and thus provides a jet which oscillates from side to side.¹²

The actual gust tunnel design involves a number of these nozzles and is shown in Fig. 1. The tunnel flow passes between the individual nozzles so that the flow actually guides the tunnel flow from side to side.

Some of the potential advantages of this method of gust generation are as follows: 1) high frequency capability; 2) low torque motors required; 3) capable of producing transverse or longitudinal gusts; 4) capable of producing various wave forms; 5) capable of producing programmed transverse disturbances; 6) capable of various phase relationships between components; and 7) capable of uniform flow across tunnel.

Presented as Paper 80-0453 at the AIAA 11th Aerodynamics Testing Conference, Colorado Springs, Colo., March 18-20, 1980; submitted April 15, 1980; revision received Feb. 12, 1981. Copyright © American Institute of Aeronautics and Astronautics, Inc., 1980. All rights reserved.

*Professor, Associate Fellow AIAA.

†Senior Research Technician.

‡Research Assistant, currently with Mead Corp., Dayton, Ohio.

The Experiment

Tunnel size limitations lead to some problems because the control valving is not as easily reduced in size as the remainder of the geometry. There is, for example, separation of the tunnel flow from the nozzle body just before the nozzle exit, if the exit velocity is very low.

The jet exit velocity is 108 m/s while the tunnel velocity is 26 m/s. The resulting jet Reynolds number based on nozzle velocity and exit size is $Re = 3.8 \times 10^4$. At an oscillation frequency of 60 Hz, the reduced frequency is $k = 0.055$ based on the nozzle spacing and an average velocity of 40 m/s.

A constant temperature hot wire anemometer is employed to survey the instantaneous velocity field. While the hot wire continuously samples the flow velocity, the signals are only recorded when the flow is in a specified orientation as determined by the rotating valve position. Thus, all data recorded with the sampling electronics at a given setting apply to the same instant in the oscillation cycle, and, effectively, the data are instantaneous (as long as the cycles are sufficiently repeatable).

Jets in Phase

As discussed in Ref. 10, the multijet tunnel is conceptually capable of producing both lateral and longitudinal gusts depending on the phase relationship between the various nozzles. If the nozzle flows are all oscillated in phase, they produce a rather large oscillation in transverse velocity (orthogonal to the mean tunnel direction). This may be seen in Fig. 2.

The instantaneous velocity distribution produced by the nozzles is shown in Fig. 2 at the instant the jet flow is in the extreme upward position. Since the distance from the nozzle exits is not large (20 nozzle exit sizes), there is still evidence of the jet nozzles in the streamwise velocity profiles. However, even this close to the exits, the velocity ratio between the peaks and valleys has been reduced from more than four at the nozzle exits to less than two. Perhaps more important is the existence of a strong lateral velocity, equal to more than 3% of the jet exit velocity or almost 10% of the local average streamwise velocity. The dashed line on the velocity profiles is the zero value before correction for a bias in the mean tunnel direction.

A similar effect is evident with the jets in the downward orientation (i.e., 180 deg phase difference). There is some shift in the streamwise velocity but an even larger effect occurs in the transverse velocity.¹² The difference in the

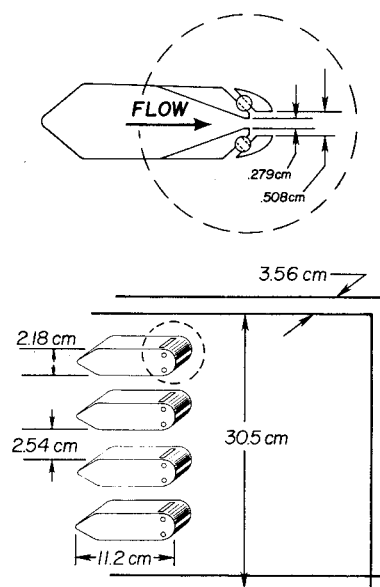


Fig. 1 Geometry of the experimental subscale pilot gust tunnel.

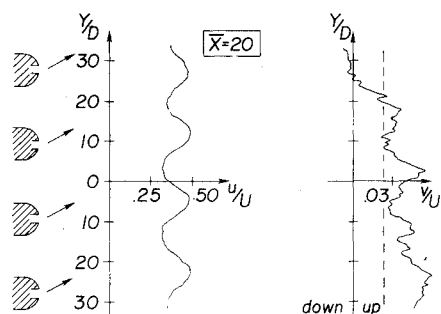


Fig. 2 Flowfield at $\bar{X}=20$ for the in-phase configuration in the upward orientation.

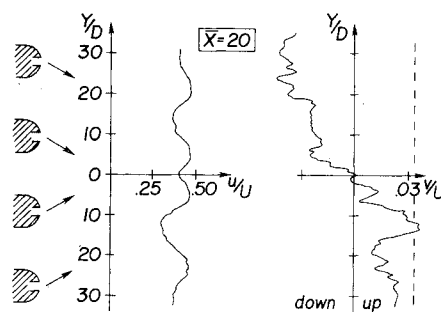


Fig. 3a Flowfield at $\bar{X}=20$ for the out-of-phase configuration and an inward orientation.

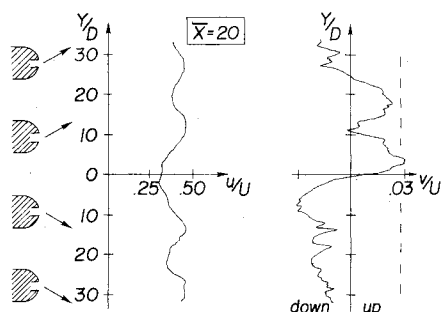


Fig. 3b Flowfield at $\bar{X}=20$ for the out-of-phase configuration and an outward orientation.

transverse component between these two particular points in the cycle, is roughly 15-20% of the mean streamwise velocity.

If the test section is moved to a position farther downstream relative to the nozzle exits, then the nonuniformity in the streamwise velocity will be rapidly reduced while the transverse oscillations with time will likewise decrease. The position of the test section is dictated, to some extent, by the fluid dynamic problem to be simulated. Farther downstream is probably best for application to aircraft gust response studies while the conditions reflected by Fig. 2 are perhaps more appropriate to the study of cascade wakes. The streamwise gust, as a percentage of the mean streamwise velocity, decays from a value of over 15% at 20 jet widths downstream to a value of 7% at 50 jet widths.

An important potential of the present gust tunnel concept is the ability to create a transverse disturbance which passes across the tunnel. As discussed in Ref. 10, such a disturbance can be generated by designing the rotating control valves in such a way as to cause the jets to periodically skip an oscillation. That is, a jet remains attached to one side while the remainder of the jets proceed through another cycle. This skipping occurs in successive nozzles on successive cycles, so the disturbance marches across the tunnel test section. This effect can then be examined as an analog to rotating stall.

However, in order to include the required changes in the control valves, the scale of the experiment must be considerably increased and thus cannot be examined with the existing apparatus.

One difficulty which appears in Fig. 2, and will also be obvious in the out-of-phase results, is the end effect of the set of nozzles. There is a finite number of nozzles in the tunnel, and since the nozzle exit velocities are larger than the tunnel velocity, the tunnel stream is actually entrained by the nozzle flow. Thus the entire set of nozzles entrains the entire tunnel flow, producing an inflow at the ends of the nozzle bank (i.e., a flow toward the center of the tunnel). The effect may be seen in the upper portion of Fig. 2 where the expected upflow is not seen but is countered by the entrained flow leading to a very small downward flow. Similar results are found at the bottom of the nozzle bank if the flow is in the downward orientation. For application, this effect may be minimized by employing a larger number of nozzles and then making use of the more central portions of the velocity field.

Jets Out of Phase

In an attempt to produce longitudinal gusts, the relative phases of the four jets are set such that the two upper jets are 180 deg out of phase with the two lower jets. The two sets of jets are then alternately aimed toward and away from each other. The flowfields corresponding to these two situations, measured at a position 20 jet thicknesses downstream, are shown in Fig. 3. In each case the transverse velocity is roughly zero at the tunnel centerline (after being corrected for the tunnel bias) and consistent with the jet orientations for positions off the tunnel axis.

Especially interesting is the possibility of using the tunnel centerline position as a test section. Comparing the centerline velocities of Fig. 3a with 3b, it is clear that a longitudinal gust of roughly 25% of the local velocity is produced.

The effect of the entrainment of the tunnel flow by the unsteady jets themselves is again evident, especially in the upper portion of Fig. 3b. There the v velocity component is expected to be positive (upward), but in fact is somewhat downward (negative), reflecting the presence of the entrainment velocity. As discussed above, this effect can be minimized by including more nozzles in the gust tunnel design, or contouring the tunnel walls.

Conclusions

Subscale experiments with a gust tunnel driven by a bank of unsteady oscillating nozzles operating in a fixed phase relationship indicate that such a device can be employed as a means to generate both lateral and longitudinal gusts. The gust percentage can be rather large, approaching 20% of the mean flow value. For smaller percentage gusts, small spatial deviations in the streamwise velocity can also be produced.

Acknowledgment

This effort was supported by the Air Force Office of Scientific Research under Grant No. 78-3525 monitored by G. Catalano, USAF, Wright Aeronautical Labs/Flight Dynamics Lab.

References

- Mitchell, C.G.B., "Assessment of the Accuracy of Gust Response Calculations by Comparison with Experiments," *Journal of Aircraft*, Vol. 7, March 1970, pp. 117-125.
- Gilman, J. Jr. and Bennett, R. M., "A Wind Tunnel Technique for Measuring Frequency Response Functions for Gust Load Analyses," *Journal of Aircraft*, Vol. 3, June 1966, pp. 535-540.
- Horlock, J. H., "An Unsteady Flow Wind Tunnel," *Aeronautical Quarterly*, Vol. 25, Part 2, May 1974.
- Ostliek, F. R., "A Cascade in Unsteady Flow—A Progress Report," *Unsteady Flows in Jet Engines, SQUID Workshop*, July 1974, edited by F. O. Carta, pp. 347-376.

⁵Sawyer, R. A., "Design and Operation of a Low Speed Gust Tunnel," AGARD CP-174, Wind Tunnel Design and Testing Techniques, London, England, Oct. 1975.

⁶Ham, N. D., Bauer, P. H., and Lawrence, T. L., "Wind Tunnel Generation of Sinusoidal Lateral and Longitudinal Gusts by Circulation Control of Twin Parallel Airfoils," Massachusetts Institute of Technology, Rept. ASRL TR 174-3, Aug. 1974.

⁷Simmons, J. M. and Platzler, M. F., "Experimental Investigation of Incompressible Flow Past Airfoils with Oscillating Jet Flaps," *Journal of Aircraft*, Vol. 8, Aug. 1971, pp. 587-592.

⁸Viets, H., "Flip-Flop Jet Nozzle," *AIAA Journal*, Vol. 13, Oct. 1975, pp. 1375-1379.

⁹Viets, H., Balster, D., and Toms, H. L. Jr., "Time Dependent Fuel Injectors," AIAA Paper 75-1305, AIAA/SAE 11th Propulsion Conference, Anaheim, Calif., 1975.

¹⁰Viets, H., "High Frequency Gust Tunnel," AGARD Conference Proceedings No. 174 on Windtunnel Design and Testing Techniques, London, England, Oct. 1975.

¹¹Piatt, M. and Viets, H., "Conditioned Sampling in an Unsteady Jet," AIAA Paper 79-1857, New York, Aug. 1979.

¹²Viets, H., Ball, M., and Piatt, M., "Experiments in a Subscale Pilot Gust Tunnel," AIAA Paper 80-0453CP, March 1980.

AIAA 81-4144

Unsteady Gas Dynamic Model of an Arc-Heated Shock Tube

Brian E. Milton*

University of New South Wales, Kensington, Australia
and

Robert E. Dannenberg†

NASA Ames Research Center, Moffett Field, Calif.

Introduction

SMALL volume, conical-shaped arc-drivers utilizing plastic diaphragms that burst concurrently with the start of the arc strike have produced high shock speeds with a simplicity of operation that is attractive.^{1,2} Because the optimization of shock-tube performance by experimental means is costly and time consuming, it would be helpful to be able to calculate the actual energy discharged within the arc chamber with the preset driver conditions necessary to achieve a desired shock speed. The gasdynamic performance and the electrical operation of arc-heated shock tubes can be predicted³ with the use of two newly developed computer codes, EGEN and ERES.⁴ EGEN calculates the maximum incident shock Mach number produced in the driven tube as a function of the time history of the energy input to the arc driver and is the subject of this Note.

EGEN Model and Program

The EGEN model was developed to examine the unsteady gasdynamics of a constant-area, arc-driven shock tube in

which the diaphragm (plastic) bursts immediately with the start of the arc discharge. The arc discharge then continues to heat that proportion of the driver gas which remains in the driver chamber, while the rest of the driver gas expands down the shock tube driving the incident shock wave. The energy addition to the gas during the discharge period referred to in this Note is that transferred by Joule heating only.⁵ It is assumed that the process is adiabatic, that the heating is spatially uniform throughout the driver chamber at any one instant, and that the heating is a function of time only. The equation of state of an ideal gas is also assumed. Viscous losses due to shock movement and irreversibilities during wave coalescence have not been considered. Also, as a first-stage solution, the length of the driven tube is not considered. It is merely assumed to be long enough in all cases for the shock reinforcement process to have given the shock its maximum value.

The unsteady gasdynamic calculations were implemented using a stepwise numerical process in which the selected energy input curve, as typified in Fig. 1a, was divided into 40 equal energy increments, the time between increments being determined from the particular curve under examination. Each increment then consisted of an instantaneous energy input followed by a short expansion period when no energy was added. Numerical investigation showed that the solution using 40 increments was within 2% of the asymptotic value when the number of increments approached infinity. There is no restriction on the size or shape of the energy input curve. The EGEN model is therefore well suited to the examination of trends relating to parametric variation of the energy input.

As the energy addition (heating) commenced, the diaphragm burst at time $t=0$ and a wave pattern formed in the usual way—a shock wave moving downstream and a rarefaction wave moving upstream. Reinforcement of this shock wave then followed due to the driver gas heating. For the chosen increments, instantaneous (i.e., constant-volume) heating allowed a pressure and a temperature rise to be calculated, using the mean driver gas mass. Using this new pressure at the diaphragm station, a matched wave system can be determined by equating the pressure and particle velocities between the two wave systems. Driver outlet pressure, temperature, and gas velocity were thereby determined; they were assumed to remain unchanged for the remaining part of the increment in which no further energy addition took place. During the latter section, constant properties at the driver exit allow the mass flow rate, and hence the total mass efflux during the time period, to be evaluated. The average gas density for the next increment was obtained by subtracting the stepwise decrement and dividing by the known driver chamber volume. The average values for the new state were found by isentropic expansion to this density.

As calculations for each increment were completed, the conditions of the gas at the driver exit were evaluated. The reinforcing process was simplified by expanding this gas isentropically until the pressure and particle velocity matched the increasing values behind the shock. For the shock, as for all EGEN code calculations, the thermodynamic properties were taken from Ref. 6; these have an upper limitation of 5000 K. In the interest of examining the general trends of the model, this temperature was substantially exceeded. Adaptation of the EGEN code, using better high-temperature thermodynamic gas properties of hydrogen, is being undertaken. Also, as an initial simplification, the ideal gas shock-wave equations were used.

The EGEN program was configured primarily to determine the final shock Mach number generated by a specified energy input. The program requires as input data the gas load conditions for the driver and driven tubes, the dimensions of the arc chamber, and the selection of the time rate and magnitude of the energy input. The computations stop if the amount of gas in the driver drops to zero before the 40 increments are completed.

Received Sept. 25, 1980; revision received Jan. 29, 1981. This paper is declared a work of the U. S. Government and therefore is in the public domain.

*Senior Lecturer, School of Mechanical and Industrial Engineering; also Ames Associate, 1977.

†Research Scientist (Ret.), presently Kendan Associates, Palo Alto, Calif. Associate Fellow AIAA.